

# Performance of the meteorological radiation model during the solar eclipse of 29 March 2006

B. E. Psiloglou and H. D. Kambezidis

Atmospheric Research Team, Institute of Environmental Research and Sustainable Development, National Observatory of Athens, Athens, Greece

Received: 6 July 2007 – Published in Atmos. Chem. Phys. Discuss.: 30 August 2007

Revised: 22 November 2007 – Accepted: 23 November 2007 – Published: 10 December 2007

**Abstract.** Various solar broadband models have been developed in the last half of the 20th century. The driving demand has been the estimation of available solar energy at different locations on earth for various applications. The motivation for such developments, though, has been the ample lack of solar radiation measurements at global scale. Therefore, the main goal of such codes is to generate artificial solar radiation series or calculate the availability of solar energy at a place.

One of the broadband models to be developed in the late 80's was the Meteorological Radiation Model (MRM). The main advantage of MRM over other similar models was its simplicity in acquiring and using the necessary input data, i.e. air temperature, relative humidity, barometric pressure and sunshine duration from any of the many meteorological stations.

The present study describes briefly the various steps (versions) of MRM and in greater detail the latest version 5. To show the flexibility and great performance of the MRM, a harsh test of the code under the (almost total) solar eclipse conditions of 29 March 2006 over Athens was performed and comparison of its results with real measurements was made. From this hard comparison it is shown that the MRM can simulate solar radiation during a solar eclipse event as effectively as on a typical day. Because of the main interest in solar energy applications about the total radiation component, MRM focuses on that. For this component, the RMSE and MBE statistical estimators during this study were found to be 7.64% and  $-1.67\%$  on 29 March as compared to the respective 5.30% and  $+2.04\%$  for 28 March. This efficiency of MRM even during an eclipse makes the model promising for easy handling of typical situations with even better results.

## 1 Introduction

The demand of exact knowledge about the availability of solar energy at different locations on the earth's surface has been increasing recently because of its use as one of the most promising renewable energy sources. Solar data, on the other hand, are nowadays used in diverse disciplines, including climatology, micro-meteorology, biology, agriculture, glaciology, urban planning, architecture, mechanical and environmental engineering. The design of many solar conversion devices, such as thermal appliances, requires the knowledge of solar radiation availability on horizontal as well as sloped surfaces. Also, the estimation of solar radiation on inclined surfaces starts with the determination of the corresponding values on horizontal plane.

It is well known that the number of the existing solar radiation stations is not adequately large throughout the world, in order to provide the required data for mapping solar radiation at a global scale. On the other hand, long-term solar radiation measurements are needed by scientists and solar energy system designers for various applications, such that the development of Solar Radiation Atlases and the generation of Typical Meteorological Years (TMYs), which are nowadays considered important tasks. Nevertheless, because of the ample lack of such data worldwide, most of the above applications must primarily rely on simulation techniques. For instance, the US National Solar Radiation Data Base provides hourly radiation data and TMYs for 239 US sites, but 93% of these data come from appropriate modeling (Maxwell, 1998; Maxwell et al., 1991).

In the context of the above, various solar radiation models (mostly broadband) have started being developed since the middle of the 20th century to calculate solar radiation components on horizontal surface, under clear sky conditions mostly. The performance of a number of broadband models tested against theoretical and measured data under clear sky conditions has been presented by Gueymard (1993a, 2003).

---

Correspondence to: B. Psiloglou  
(bill@meteo.noa.gr)

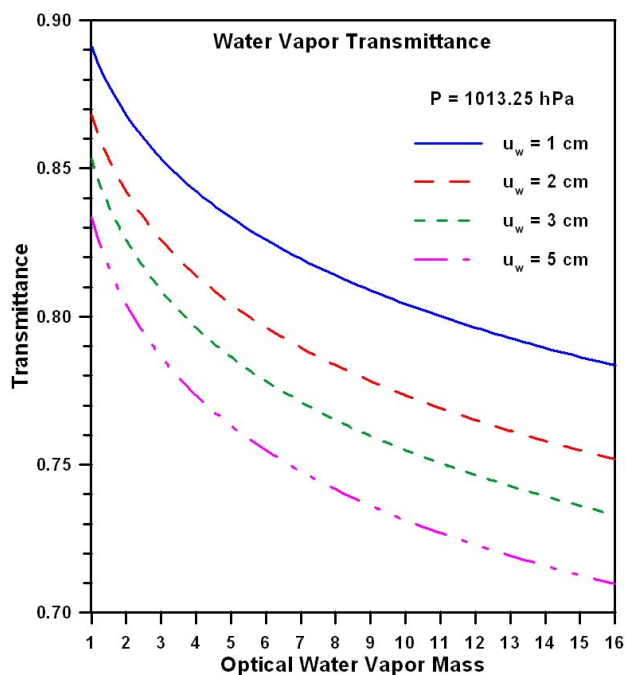


**Fig. 1.** Water vapor absorption transmittance for different values of  $u_w$ , as predicted by MRM v5.

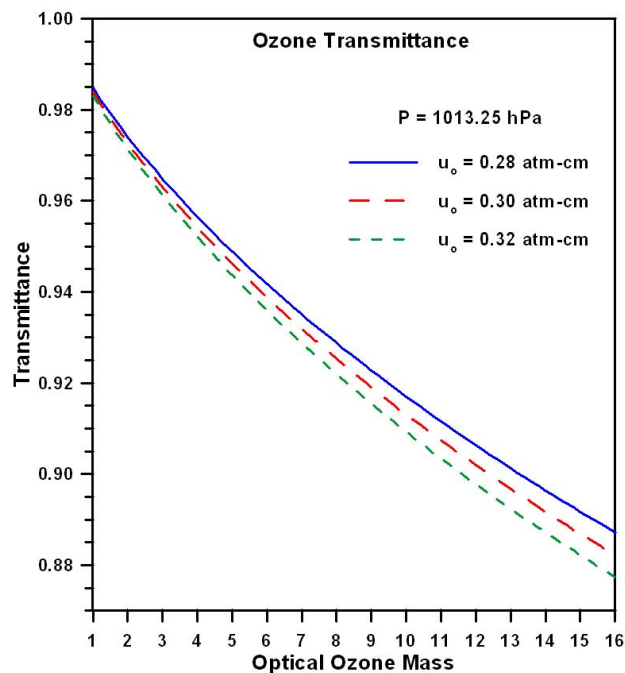


**Fig. 2.** Ozone absorption transmittance for different values of  $u_o$ , as predicted by MRM v5.

The Atmospheric Research Team (ART) at the National Observatory of Athens (NOA) has developed the so-called Meteorological Radiation Model, or MRM in brevity (Kambezidis and Papanikolaou, 1989, 1990a; Kambezidis et al., 1993; Kambezidis et al., 1997). The initiative of this development was to derive solar radiation data for places where these are not available because of lack of such measurements. To do that, the MRM employed meteorological data only (viz. air temperature, relative humidity, barometric pressure and sunshine duration) that are available worldwide.

The MRM code passed through different phases of development since its first version. Its latest version is 5. The original form of MRM (MRM v1) worked efficiently under clear sky conditions, but it could not work under partly cloudy or overcast skies. MRM v2 introduced new analytical transmittance equations and, therefore, became more efficient than its predecessor. Nevertheless, this version still worked well under clear sky conditions only. These deficiencies were resolved via the development of MRM v3, derived by T. Muneer's research group at Napier University, Edinburgh (Muneer et al., 1996; Muneer, 1997; Muneer et al., 1997; Muneer et al., 1998) after successful co-operation between ART and his group. MRM v3 was included in the book edited by Muneer (1997). Through the EC JOULE III project on Climatic Synthetic Time Series for the Mediterranean Belt (acronym: CliMed), a further development of the MRM was achieved, which is referred to as version four (MRM v4), providing further improvement in relation

with the partly cloudy and overcast skies. The algorithm of MRM v4 was used by Prof. Hassid, Technion University, Israel, to make simulations and comparison with Israeli solar radiation data (unpublished work). In using the code, he found some errors mainly in the calculation of the daily solar course in the sky; these errors were later incorporated in the algorithm. On the other hand, Gueymard (2003), in an inter-comparison study employing various broadband models, used MRM v4 and found it not to be performing so well in relation to others. These tests forced ART to reconsider the source code of MRM. The effort resulted in discovering further errors in the transmittance and solar geometry functions; new transmittance and more effective solar geometry functions were, therefore, introduced from the international literature concluding to MRM v5. Also the recent solar constant of  $1366.1 \text{ W m}^{-2}$  was incorporated in version 5.

It must be emphasized here that MRM is capable in performing calculations in various time steps, i.e. from one hour to one minute. This is dictated by the availability of the meteorological input data. The majority of them are provided on hourly basis. Nevertheless, there are stations rendering data as average values less than hourly, e.g. 5-min or 1-min values. On the other hand, the measured sunshine duration, another input parameter to MRM, is usually given as either a total daily or hourly value. In the last case, provided that the meteorological data are given as 1-min average values, the MRM can derive more precise calculations. MRM has successfully been used by the

Chartered Institution of Building-Service Engineers (CIBSE) of UK under the Solar Data Task Group in 1994 (Muneer, 1997). Apart from that specific task, MRM can be used in a variety of applications, among of which the most important nowadays are:

1. to estimate solar irradiance on horizontal plane to be used as input parameter to codes calculating solar irradiance on inclined surfaces with arbitrary orientation,
2. to estimate solar irradiance on horizontal plane with the use of available meteorological data for deriving the solar climatology at a location,
3. to fill gaps of missing solar radiation values in a series of historic data from corresponding observations of available meteorological parameters,
4. to provide results for engineering purposes, e.g. solar-energy applications, PV efficiency, energy-efficient buildings and daylight applications.

The primary objective of this study was to test the performance of the new version of MRM during the recent solar eclipse of 29 March 2006. Nevertheless, such a simulation by a broadband model during an eclipse event is the first to appear in the international literature because of the difficulty to describe correctly the atmospheric conditions and solar geometry during the phase of the eclipse within the code. The results of this study have, however, a scientific and not a practical value, but can justify the performance of MRM v5 under very “adverse conditions” as those of a solar eclipse. The sun’s disk coverage during the eclipse maximum on 29 March 2006 was 84% at the Actinometric Station of NOAA (ASNOA) featuring an almost total eclipse. For comparison, the performance of the model was also tested during the preceding day of the eclipse, i.e. 28 March 2006. In the present study, 1-min values of meteorological parameters and sunshine duration were used. A full description of the code is given in Sect. 2.

## 2 Model description

MRM is a broadband algorithm for simulation and estimation of solar irradiance on horizontal surface, using widely available meteorological information, viz. values of air temperature, relative humidity, barometric pressure, and sunshine duration as input parameters. This Section provides a detailed description of the newly developed MRM, version 5, incorporating all recent knowledge on the subject.

As mentioned in the Introduction, MRM is flexible in estimating hourly to even 1-min radiation values; this flexibility solely depends upon the time step of the input parameters. It is absolutely understandable that the choice of 1-min values for the input data (including sunshine duration  $n$ ) into the code makes MRM more efficient, since solar radiation estimations are then given in high temporal resolution.

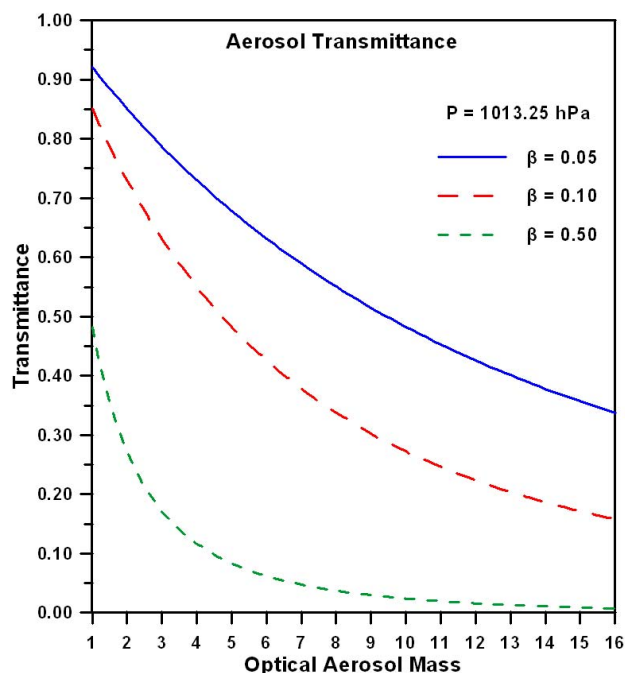


Fig. 3. Total aerosol extinction transmittance for different values of  $\beta$ , as predicted by MRM v5.

### 2.1 Clear sky MRM sub-model

#### 2.1.1 Direct beam radiation

The direct beam component of solar radiation (the radiation arriving directly from the sun) normal to a horizontal plane at the earth’s surface, under clear sky and natural (without anthropogenic influence) atmosphere, is the extra-terrestrial radiation at the top of the atmosphere modified by the absorption and scattering from its various constituents. Thus, during cloudless periods, the direct beam radiation,  $I_b$ , received on a horizontal surface can be expressed as:

$$I_b = I_{ex} \cos \theta_z T_w T_r T_o T_{mg} T_a \quad (1)$$

where  $\theta_z$  is the solar zenith angle,  $I_{ex}$  is the normal incidence extra-terrestrial solar radiation on the  $n_i$ -th day of the year; the  $T$  terms are the broadband transmission functions for water vapor ( $T_w$ ), Rayleigh scattering ( $T_r$ ), uniformly mixed gases ( $\text{CO}_2$ ,  $\text{CO}$ ,  $\text{N}_2\text{O}$ ,  $\text{CH}_4$  and  $\text{O}_2$ ) absorption ( $T_{mg}$ ), ozone absorption ( $T_o$ ), and aerosol total extinction (scattering and absorption) ( $T_a$ ).

The general transmittance function,  $T_i$ , for seven main atmospheric gases ( $\text{H}_2\text{O}$ ,  $\text{O}_3$ ,  $\text{CO}_2$ ,  $\text{CO}$ ,  $\text{N}_2\text{O}$ ,  $\text{CH}_4$  and  $\text{O}_2$ ) can be expressed by the following equation (Psiloglou et al., 1994, 1995a, 1996, 2000):

$$T_i = 1 - \frac{a m u_i}{(1 + b m u_i)^c + d m u_i} \quad (2)$$

**Table 1.** Values of the coefficients  $a$ ,  $b$ ,  $c$  and  $d$  in the general transmittance function of Eq. (2) for various atmospheric constituents.

Atmospheric constituent	$a$	$b$	$c$	$d$
H <sub>2</sub> O	3.0140	119.300	0.6440	5.8140
O <sub>3</sub>	0.2554	6107.26	0.2040	0.4710
CO <sub>2</sub>	0.7210	377.890	0.5855	3.1709
CO	0.0062	243.670	0.4246	1.7222
N <sub>2</sub> O	0.0326	107.413	0.5501	0.9093
CH <sub>4</sub>	0.0192	166.095	0.4221	0.7186
O <sub>2</sub>	0.0003	476.934	0.4892	0.1261

where  $m$  is the optical air mass, and  $a$ ,  $b$ ,  $c$ ,  $d$  are numerical coefficients that depend on the specific extinction process; the values of these coefficients are given in Table 1.

The optical air mass,  $m$ , at standard pressure conditions, is given by Kasten and Young (1989):

$$m = [\cos \theta_z + 0.50572(96.07995 - \theta_z)^{-1.6364}]^{-1}. \quad (3)$$

This above formula is accurate for all  $m$ 's up to  $\theta_z < 85^\circ$  with an error of less than 0.5%. The pressure-corrected air mass,  $m'$ , can then be estimated by the expression:

$$m' = m \left( \frac{P}{P_o} \right) \quad (4)$$

where  $P$  is the atmospheric pressure at the station's height, in hPa, and  $P_o = 1013.25$  hPa the mean atmospheric pressure at sea level. The  $m$  has been used here only for ozone, water vapor and aerosols, whereas the  $m'$  is used for the Rayleigh scattering and mixed gases absorption.

In Eq. (2),  $u_i$  represents the "absorption amount in a vertical column" for each extinction process. This quantity is variable for water vapor and ozone, and represented by  $u_w$  (in atm-cm) and  $u_o$  (in atm-cm), respectively. The necessary  $u_i$  values (in atm-cm) for the other atmospheric gases of Table 1 are: 1.60 for CH<sub>4</sub>, 0.075 for CO, 350.0 for CO<sub>2</sub>, 0.28 for N<sub>2</sub>O, and  $2.095 \times 10^5$  for O<sub>2</sub>.

For the estimation of the water vapor total amount in a vertical column (the so-called precipitable water), the following expression (Leckner, 1978) is used:

$$u_w = \frac{0.493 e_m}{T} \quad (5)$$

where  $e_m$  is the partial water vapor pressure, in hPa, given by:

$$e_m = e_s \left( \frac{RH}{100} \right) \quad (6)$$

where RH is the relative humidity at the station's height, in %, and  $e_s$  is the saturation vapor pressure, in hPa, given by

Gueymard (1993b):

$$e_s = \exp(22.329699 - 49.140396 T_1^{-1} - 10.921853 T_1^{-2} - 0.39015156 T_1) \quad (7)$$

with  $T_1 = T/100$ ,  $T$  being the air temperature at the station's height, in K.

The broadband transmittance function due to the total absorption by the uniformly mixed gases can then be calculated by:

$$T_{mg} = T_{CO_2} T_{CO} T_{N_2O} T_{CH_4} T_{O_2} \quad (8)$$

where the transmittances  $T_{CO_2}$ ,  $T_{CO}$ ,  $T_{N_2O}$ ,  $T_{CH_4}$  and  $T_{O_2}$  are given by Eq. (2) using the appropriate coefficients of Table 1.

The transmittance corresponding to the Rayleigh scattering is calculated from Psiloglou et al. (1995b):

$$T_r = \exp[-0.1128 m^{0.8346} (0.9341 - m^{0.9868} + 0.9391 m')] \quad (9)$$

Very few locations in the world provide detailed aerosol data. In general, solar radiation modelers are forced to use or develop aerosol models specific for their own site of application. In the present study, the Mie scattering transmittance function proposed by Yang et al. (2001) has been incorporated in MRM v5:

$$T_a = \exp\{-m\beta[0.6777 + 0.1464m\beta - 0.00626(m\beta)^2]^{-1.3}\} \quad (10)$$

where the Ångström's turbidity parameter,  $\beta$ , is in the range 0.05–0.4 for low-to-high aerosol loads. Some indicative values of  $\beta$  are given in Table 2 (Iqbal, 1983).

Another way of estimating  $\beta$ , when not available from measurements, is by using the Yang et al.'s (2001) expression, which relates  $\beta$  to the geographical latitude,  $\phi$ , and the altitude of the station,  $H$ . This expression is:

$$\beta = \beta' + \Delta\beta \quad (11)$$

$$\beta' = (0.025 + 0.1 \cos \phi) \exp\left(\frac{-0.7 H}{1000}\right) \quad (12)$$

$$\Delta\beta = \pm(0.02 \sim 0.06) \quad (13)$$

where  $\beta'$  represents the annual mean value of turbidity and  $\Delta\beta$  the seasonal deviation from the average, i.e. low values in winter, high values in the summer. For Athens ( $\phi = 37.967^\circ$  N,  $H = 107$  m a.m.s.l.)  $\beta' = 0.09$ .

During the earth's movement around the sun,  $I_{ex}$  varies by approximately  $\pm 3.5\%$  of its value at the equinoxes.  $I_{ex}$  may be expressed on the  $n_i$ -th day of the year as (Spencer, 1971):

$$I_{ex} = I_o [1.00011 + 0.034221 \cos \Gamma + 0.00128 \sin \Gamma + 0.000719 \cos 2\Gamma + 0.000077 \sin 2\Gamma] \quad (14)$$

where  $I_o$  is the solar constant, equal to  $1366.1 \text{ W m}^{-2}$ , and  $\Gamma$  (in rad) is the day angle, which is given by:

$$\Gamma = \frac{2\pi(n_i - 1)}{365} \quad (15)$$

**Table 2.** Indicative values of the Ångström's turbidity parameter,  $\beta$ , for various atmospheric conditions and horizontal visibilities,  $V$ .

Atmospheric condition	$\beta$	$V$ (km)
Clean	0.05	340
Clear	0.10	28
Turbid	0.20	11
Very turbid	0.40–0.50	<5

where the day number of the year,  $n_i$ , ranges from 1 (1 January) to 365 (31 December); February is always assumed to have 28 days.

Figures 1–3 show the transmittances of water vapor, ozone and total aerosol extinction, respectively, as predicted by the new MRM v5 algorithm.

### 2.1.2 Diffuse radiation

Under clear sky conditions, the diffuse (indirect) sky radiation is assumed to be made up of a portion of singly scattered by the atmospheric constituents (molecules and aerosol particles) direct beam radiation,  $I_{ds}$ , plus a multiple scattering component,  $I_{dm}$  (Atwater and Brown, 1974; Psiloglou et al., 2000):

$$I_{ds} = I_{ex} \cos \theta_z T_w T_{mg} T_o T_{aa} 0.5(1 - T_{as} T_r) \quad (16)$$

The first part in the right hand side of Eq. (16), i.e.  $I_{ex} T_w T_{mg} T_o T_{aa}$ , represents the amount of solar radiation left over after its absorption by the atmospheric constituents and aerosols, while the second part, i.e.  $0.5(1 - T_{as} T_r)$ , expresses the amount of solar radiation scattered forward (towards the surface of the earth) by air molecules and aerosol particles.

The aerosol transmittance function due to absorption only,  $T_{aa}$ , is given by the expression (Bird and Hulstrom, 1980; 1981):

$$T_{aa} = 1 - 0.1(1 - m + m^{1.06})(1 - T_a) \quad (17)$$

and the aerosol transmittance due to scattering alone,  $T_{as}$ , can be estimated from:

$$T_{as} = \frac{T_a}{T_{aa}} \quad (18)$$

The diffuse component, which is due to a single reflection of  $I_b$  and  $I_{ds}$  from the earth's surface, followed by backscattering from the atmospheric constituents,  $I_{dm}$ , is modeled as:

$$I_{dm} = (I_b + I_{ds}) \frac{\alpha_g \alpha_s}{1 - \alpha_g \alpha_s} \quad (19)$$

where  $\alpha_g$  is the surface albedo, usually taken to be equal to 0.2, and  $\alpha_s$  the albedo of the cloudless sky. The atmospheric

albedo is defined as the ratio of the energy reflected back to space to the incident one. Under clear sky conditions, it can be approximated using the following form:

$$\alpha_s = \alpha_r + \alpha_a \quad (20)$$

where  $\alpha_r$  represents the albedo due to the molecular (Rayleigh) scattering, commonly taken to be equal to 0.0685 after Lacis and Hansen (1974).

The second term,  $\alpha_a$ , is the atmospheric aerosol albedo due to the atmospheric aerosol scattering, and can be estimated from the following equation (Bird and Hulstrom, 1980; 1981):

$$\alpha_a = 0.16(1 - T_{a,1.66}) \quad (21)$$

where  $T_{a,1.66}$  implies the value of the total aerosol transmittance,  $T_a$ , calculated for  $m=1.66$  (i.e. for  $\theta_z=53^\circ$ ).

The diffuse radiation at ground level under clear sky conditions,  $I_d$ , is then simply the sum of the  $I_{ds}$  and  $I_{dm}$  components, i.e.:

$$I_d = I_{ds} + I_{dm} \quad (22)$$

### 2.1.3 Total radiation

The total solar radiation,  $I_t$ , received under clear sky conditions on horizontal plane at the surface of the earth is simply the sum of the horizontal components  $I_b$  from Eq. (1), and  $I_d$  from Eq. (22), i.e.:

$$I_t = I_b + I_d = \frac{I_b + I_{ds}}{1 - \alpha_g \alpha_s} \quad (23)$$

## 2.2 Cloudy sky MRM sub-model

Clouds play an important role in modifying radiation as they significantly affect the reflectance, absorptance and transmittance of the incident radiation. However, the present understanding of their effect on solar radiation is at a good level, but its modeling in the various radiative models (broadband or spectral) is far from being efficient and lies on statistical techniques than physical processes (Konratyev, 1969; Davies et al., 1975; Suckling and Hay, 1977; Barbaro et al., 1979; Munro, 1991; Gu et al., 2001; Badescu, 2002; Ehnberg and Bollen, 2005). The direct beam radiation is attenuated by the presence of clouds by blocking its propagation through the atmosphere, as well as by the various atmospheric constituents, as already discussed above. The depletion of the direct beam component by clouds depends on their type, thickness, and number of layers.

The diffuse component consists of several parts. The mechanism of scattering by air molecules and aerosols is the same with the one already described above. In addition, there is an interaction between the direct beam solar radiation and clouds, resulting in reflected diffuse radiation. Further, a portion of the direct beam and diffuse radiation components reaching the surface of the earth is reflected back to

**Table 3.** Typical values of  $k^*$  as proposed by Berland and Danilchenko (1961) for different latitudes.

$k^*$	$\phi$ (deg)
0.32	30
0.32	35
0.33	40
0.34	45

space; this part contributes to a multiply reflected irradiance. This latter radiation component depends strongly on the reflectance properties of the clouds system. When the sky is completely overcast, the diffuse component is considered almost isotropic.

Theoretical determinations of the direct beam and diffuse irradiance components under cloudy sky conditions are quite difficult. Such tasks require detailed data on the type and optical properties of clouds, cloud coverage, thickness, position and number of layers. Such data are very rarely collected on a routine basis.

However, several methods have been developed to model solar radiation under cloudy skies. Depending on the type of input data used for each model, Davies et al. (1984) identified five model groups: (i) sunshine based models, (ii) cloud layer based models, (iii) total cloud based models, (iv) satellite data based models, and (v) Liu-Jordan (1960) type models; all these groups discriminate total radiation into direct beam and diffuse components.

In the last version of MRM, an algorithm for calculating the solar radiation components on cloudy days has been introduced. Given the absence of adequate information on cloudiness, solar radiation is simulated by MRM using the measured sunshine duration,  $n$ , which is widely measured and easily available to most users from existing national meteorological stations.

### 2.2.1 Direct beam radiation

The direct beam solar radiation under clear skies,  $I_b$ , decreases in the presence of clouds by the factor  $T_c$ , which depends on the characteristics of cloudiness (Barbaro et al., 1979). Therefore, the direct beam solar radiation under cloudy skies,  $I_{cb}$ , can be obtained by:

$$I_{cb} = I_b T_c \quad (24)$$

where  $T_c$  is the cloud transmittance, and  $I_b$  is calculated from Eq. (1).

Generally,  $T_c$  can be expressed as a function of the relative sunshine duration,  $n/N$ , which is the ratio of the daily measured sunshine duration,  $n$ , to its maximum (astronomical) value,  $N$ :

$$T_c = k \left( \frac{n}{N} \right) \quad (25)$$

where  $k$  is an empirical coefficient for cloudiness with a usual value equal to unity. Such an approximation, as that in Eq. (24), is necessary because the information pertaining to cloudiness is unsatisfactory.

Barbaro (1979) allows  $k=1$ , but Ideriah (1981) proposed a value of  $k=0.75$  to provide better agreement between estimates and measurements. For the Athens data  $k$  was found to vary between 0.85 and 0.95 for the winter months, and be 1.0 for the summer period (Psiloglou et al., 2000).

### 2.2.2 Diffuse radiation

The single scattered portion of the diffuse radiation in the presence of clouds,  $T_{cds}$ , can be computed by Barbaro et al. (1979):

$$I_{cds} = I_{ds} T_c + k^* (1 - T_c) (I_b + I_{ds}) \quad (26)$$

where  $k^*$  is an empirical transmission coefficient, whose value is a function of  $\phi$ , and is obtained from Berland and Danilchenko (1961). Values of  $k^*$  are given in Table 3 for different latitudes. For the case of Athens ( $\phi=37.967^\circ$  N), the value of  $k^*=0.33$  has been adopted (see Table 3).

The ground reflected, atmospheric and cloud backscattered diffuse term,  $I_{cdm}$ , is modeled identically as in clear sky conditions:

$$I_{cdm} = (I_{cb} + I_{cds}) \frac{\alpha_g \alpha_{cs}}{1 - \alpha_g \alpha_{cs}} \quad (27)$$

where  $\alpha_{cs}$  is the albedo of the cloudy sky.

In order to estimate the atmospheric albedo of a cloudy sky, a corrective factor for multiple scattering between the clouds and the surface of the earth,  $\alpha_c$ , is introduced in Eq. (20). Thus the new formula is expressed as:

$$\alpha_{cs} = \alpha_r + \alpha_a + \alpha_c \quad (28)$$

where the  $\alpha$ 's in the right hand side of Eq. (28) are defined for clear skies (see Eqs. 20, 21);  $\alpha_c$  is given by various analytical expressions (Atwater and Ball, 1978; Davies and McKay, 1982; Lyons and Edwards, 1982), as a function of  $n$ . In MRM v5, the following expression has been adopted:

$$\alpha_c = \nu \left( 1 - \frac{n}{N} \right) \quad (29)$$

where  $\nu$  is a parameter varying between 0.3 and 0.6. For Athens, the value of  $\nu=0.4$  was found to be more appropriate (Psiloglou et al., 2000).

Therefore, the diffuse radiation at ground level under cloudy skies,  $I_{cd}$ , is the sum of the  $I_{cds}$  and  $I_{cdm}$  components, i.e.:

$$I_{cd} = I_{cds} + I_{cdm} \quad (30)$$

### 2.2.3 Total radiation

The total solar radiation received under cloudy sky conditions (partly or overcast) on horizontal surface is the sum of the horizontal direct beam and diffuse components, i.e.:

$$I_{ct} = I_{cb} + I_{cd} = \frac{I_{cb} + I_{cds}}{1 - \alpha_g \alpha_{cs}} \quad (31)$$

## 3 Validation of MRM v5

### 3.1 Data collection and quality test

In order to evaluate the performance of the newly introduced version 5 of the MRM algorithm under normal and extraordinary conditions, 1-min mean total and diffuse horizontal solar irradiance data ( $\text{Wm}^{-2}$ ) from ASNOA were used together with concurrent values of dry bulb temperature, relative humidity, sunshine duration, and atmospheric pressure at the station's height from the meteorological station of NOA, for 28 (typical clear day) and 29 (eclipse day) March 2006.

NOA ( $37.967^\circ \text{N}$ ,  $23.717^\circ \text{E}$ ) is located on the hill of Pnyx (107 m a.s.l.) near the Athens city center. The Athens Metropolitan area is located in the central part of the Attica Peninsula in an oblong basin having a NE-SW direction; the basin has an area of  $450 \text{ km}^2$  and is inhabited by 3.5 millions of people (census of 2001). To the east of the basin's axis, the city is less densely populated. To the west, the area is industrial and residential. The average annual sunshine duration is 2919 h.

The actinometers for measuring total and diffuse horizontal radiations at ASNOA are Eppley PSP pyranometers; the diffuse radiation is measured using an Eppley shadow band. Up to now no shadow ring corrections have been applied to the ASNOA diffuse measurements because of lack of simultaneous direct beam measurements. Very recently ASNOA put in operation an automatic sun tracker carrying four pyrhemometers for measuring the direct beam components in various optical bands as well the total one. After the collection of sufficient statistically sound solar data a comparison of the normal diffuse values with those accruing from the difference of total and direct beam components will be made. Then, the best suited of the several existing methodologies in the international literature for correcting diffuse data for the shadow band effect will be chosen.

To establish a valid set of measurements for the validation of the MRM code, the 1-min mean total and diffuse horizontal irradiance values were thoroughly tested for errors. A routine quality control procedure was applied; all erroneous data were excluded. The quality tests screened out all (i) diffuse horizontal values greater than 110% of the corresponding total horizontal ones; (ii) total horizontal values greater than 120% of the seasonally correct solar constant; (iii) diffuse horizontal values greater than 80% of the seasonally correct solar constant; (iv) total horizontal values equal to or less

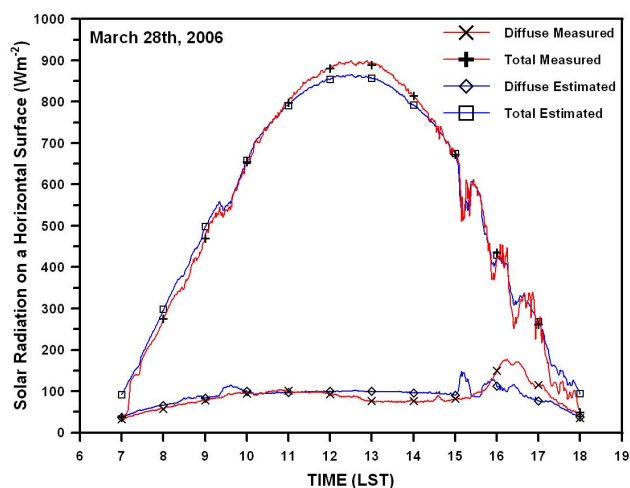


Fig. 4a. Comparison between MRM simulations (blue lines) and measurements (red lines) for Athens on 28 March 2006.

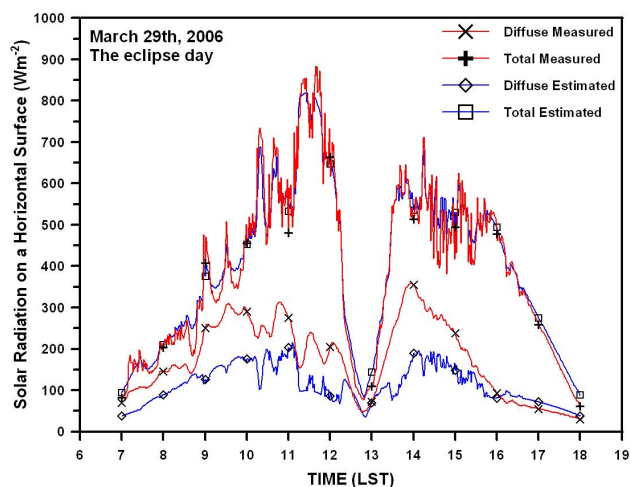


Fig. 4b. As in Fig. 4a, but on 29 March 2006.

than  $5 \text{ Wm}^{-2}$ , during sunrise and sunset, due to the pyranometers' sensitivity; (v) data for solar altitude less than  $5^\circ$ ; and (vi) data with the direct beam solar component exceeding the extraterrestrial solar irradiance. Thus, 661 1-min data points passed the quality control tests, for each day (28 and 29 March 2006).

It must be noted here that during the eclipse phenomenon, from its start to its end,  $I_{ex}$  was multiplied by the factor 1-EM, where EM stands for the eclipse magnitude, i.e. the fraction of the solar disk covered by the moon's shadow. This was done in order to simulate the phenomenon in the MRM algorithm.

As said before, 1-min values for the meteorological input data were chosen to be used in the MRM algorithm. This confined  $n$  to the same accuracy. Because of unavailability

**Table 4.** Evolution of the eclipse magnitude (EM) over Athens on 29 March 2006 from the start to its maximum. The time is counting from the moment just before the start of the phenomenon.

Time (min)	EM	Time (min)	EM	Time (min)	EM	Time (min)	EM
0	0.0000	20	0.1253	40	0.3411	60	0.6008
1	0.0015	21	0.1346	41	0.3533	61	0.6146
2	0.0041	22	0.144	42	0.3655	62	0.6283
3	0.0075	23	0.1537	43	0.3779	63	0.6422
4	0.0115	24	0.1635	44	0.3903	64	0.6560
5	0.0161	25	0.1736	45	0.4030	65	0.6700
6	0.0211	26	0.1837	46	0.4155	66	0.6839
7	0.0266	27	0.1941	47	0.4283	67	0.6980
8	0.0324	28	0.2045	48	0.4411	68	0.7120
9	0.0386	29	0.2152	49	0.4541	69	0.7261
10	0.0451	30	0.2259	50	0.4670	70	0.7402
11	0.0520	31	0.2369	51	0.4801	71	0.7544
12	0.0591	32	0.2479	52	0.4932	72	0.7686
13	0.0665	33	0.2592	53	0.5065	73	0.7828
14	0.0742	34	0.2705	54	0.5197	74	0.7970
15	0.0822	35	0.2820	55	0.5331	75	0.8114
16	0.0903	36	0.2936	56	0.5465	76	0.8256
17	0.0988	37	0.3053	57	0.5601	77	0.8400
18	0.1074	38	0.3171	58	0.5736		
19	0.1163	39	0.3291	59	0.5872		
continued	↑	continued	↑	continued	↑		

of such sunshine duration values at ASNOA, a method was developed to fill the gap. A polynomial function was fitted to the total solar radiation curve of 28 March, an almost perfect clear day. The same function was checked on previous clear days prior and close to 28 March to assure its shape as best fit to the measured values. This fit was used on 29 March after applying the factor 1-EM to simulate the eclipse event. On both days,  $n$  was calculated as the ratio of the measured to the “fitted” radiation values using 1-min time steps. If the ratio was greater than one,  $n$  was then set equal to unity. In this way, the detailed fluctuations of the radiation components were reproduced correctly in a qualitative manner. To make sure that the method is right, the measured daily sunshine duration at ASNOA on both days was compared to the summation of all estimated 1-min sunshine duration values. The agreement was almost perfect.

The value of  $u_o$  in the MRM code can either be calculated through the Van Heuklon (1979) methodology or be given in atm-cm from available satellite or ground based instruments. In the present study, the value of  $u_o$  was obtained from a Brewer spectrophotometer operating in the center of Athens (Academy of Athens). No matter which of the above mentioned methodologies is used, the  $u_o$  value is introduced in the MRM as an average daily value. These average daily values were 279.8 and 316.9 DU (1 atm-cm=1 DU $\times 10^{-3}$ ) for 28 and 29 March 2006, respectively.

According to NOAA’s records, similar weather conditions prevailed on both 28 and 29 March, namely unaltered wind speeds and directions. As no measurements of the Ångström’s turbidity parameter,  $\beta$ , were available, the 28 March 2006 (one day before the eclipse with almost clear sky) was selected for reference. By using Eq. (12) with  $H=107$  m, the value of  $\beta'$  was found equal to 0.09. Some tests were, then, carried out by varying the value of  $\Delta\beta$  in the range 0.02–0.06, as proposed by Yang et al. (2001). The best MRM results concerning both the total and diffuse components on the 28 March were found with the value of  $\Delta\beta=-0.04$ . Therefore, the value of  $\beta=0.05$  was found from Eq. (11) and was used for both the pre-eclipse and eclipse days.

The calculations of the solar position in the sky on both dates (prior and during the eclipse) were performed using the modified SUNAE algorithm (Walraven, 1978), incorporating all corrections introduced by Wilkinson (1981), Muir (1983), Kambezidis and Papanikolaou (1990b), and Kambezidis and Tsangrassoulis (1993).

Table 4 gives the 1-min values of EM during the eclipse day. The start of the eclipse is taken at 0 min (11:30 h LST) in the left column of the Table corresponding to the last minute before the beginning of the sun’s disk blockage by the moon. The maximum of the eclipse was for Athens 84% at 12:48 h LST. The descending limb of the phenomenon

lasted 77 min and the whole phenomenon 154 min, i.e. from 11:30 h LST to 14:04 h LST.

### 3.2 Statistical analysis

The Root Mean Square Error (RMSE) and the Mean Bias Error (MBE), both in  $\text{Wm}^{-2}$  and in % of the measured mean value, were used as indicators of the model's performance:

$$\text{RMSE (in } \text{Wm}^{-2}\text{)} = \sqrt{\frac{\sum_{i=1}^M (I_m - I_c)^2}{M}} \quad (32)$$

$$\text{MBE (in } \text{Wm}^{-2}\text{)} = \frac{\sum_{i=1}^M (I_m - I_c)}{M} \quad (33)$$

$$\text{RMSE (in \%)} = \frac{\text{RMSE (in } \text{Wm}^{-2}\text{)}}{\frac{\sum_{i=1}^M I_m}{M}} \times 100 \quad (34)$$

$$\text{MBE (in \%)} = \frac{\text{MBE (in } \text{Wm}^{-2}\text{)}}{\frac{\sum_{i=1}^M I_m}{M}} \times 100 \quad (35)$$

where  $I_m$  and  $I_c$  are the measured and model estimated values of the total or diffuse radiation (in  $\text{Wm}^{-2}$ ) and  $M=661$  is the number of data points on each of the two dates. The values of these estimators, in  $\text{Wm}^{-2}$ , for the total and diffuse horizontal radiation components along with their mean daily measured values for both dates are given in Table 5. The brackets in the RMSE and MBE columns indicate their values in %.

The comparison between the MRM modeled radiation components (total and diffuse) and the measured ones for the day before the eclipse is shown in Fig. 4a. A very good agreement is observed that is also obvious from the statistical estimators in Table 5. For the clear part of the day on 28 March, it can be seen from Fig. 4a that MRM slightly overestimates the values of the total solar radiation during the early morning and late afternoon hours, but it slightly underestimates it during the central hours of the day. This discrepancy may be attributed to a local variation in the aerosol synthesis and concentration, factors that cannot be simulated properly in the MRM code with a single value of  $\beta$  the whole day. On the other hand, the diffuse radiation shows similar behavior during the clear part, but this is not the case in the second half of the day when cirrus clouds appeared over ASNOA. On 29 March (Fig. 4b), MRM continuously underestimated the diffuse radiation. This can be attributed to the general observation that no radiation code up to now can simulate the effect of clouds on solar radiation in a precise manner. No matter what methodology is used, the extra diffuse radiation produced under cloudy skies is still unknown for the various types of clouds. The methodology detailed in Sect. 3.1

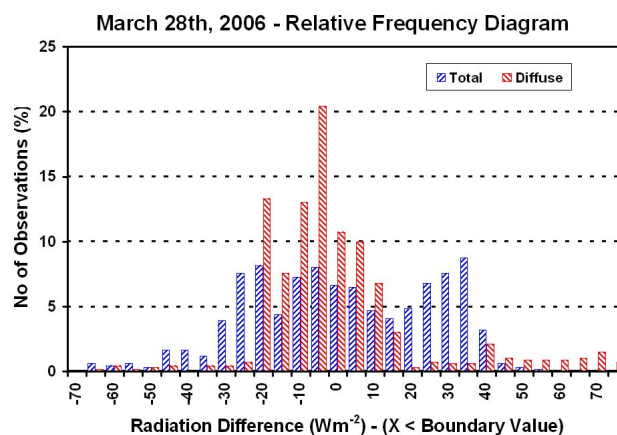


**Fig. 5a.** Relative frequency distribution (in %) of the differences between the measured and MRM estimated total and diffuse radiation components (in  $\text{Wm}^{-2}$ ) for Athens on 28 March 2006.

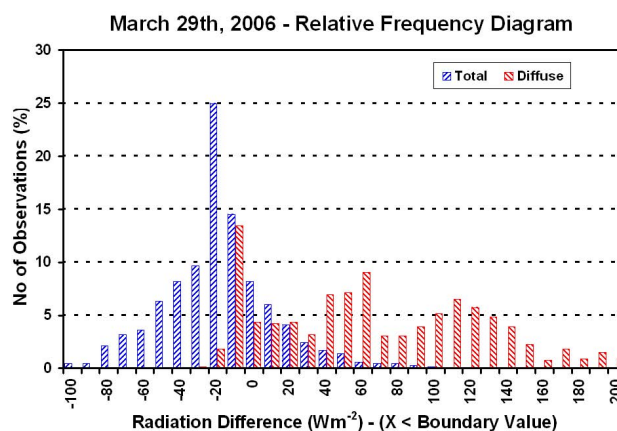


**Fig. 5b.** As in Fig. 5a, but for 29 March 2006.

for the derivation of the 1-min sunshine duration values managed, though, to describe the effect of clouds on solar radiation on the eclipse day in a very efficient and qualitative manner.

In order to have a better understanding of the performance of the MRM, the differences between the measured and estimated values for both the total and diffuse radiation components were calculated. Figure 5a and b show the relative frequency (in %) of the distribution of the above differences for both 28 and 29 March. It is interesting to observe the nearly equal distribution of the differences for the total component on both days around  $0 \text{ Wm}^{-2}$ . This occurs because the overestimations (negative differences) are almost equal in absolute terms to the underestimations (positive differences) of the MRM simulations. Indeed, the MBE statistical estimator was  $-1.67\%$  on 29 March for the simulated total solar radiation in comparison with the respective  $+2.04\%$  on the preceding clear day. To the contrary, the respective distribution of

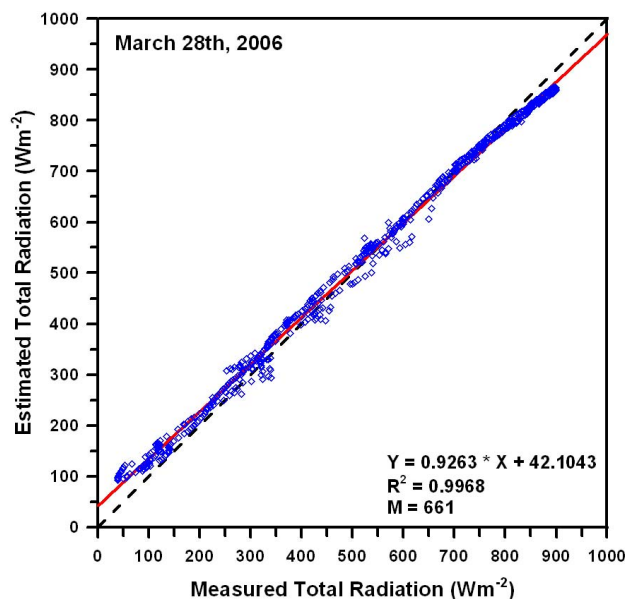


**Fig. 6a.** Estimated vs. measured values of total solar radiation on horizontal surface for Athens on 28 March 2006. The best fit equation (red line), the determination coefficient value ( $R^2$ ) and the number of available data ( $M$ ) are also given. The  $y=x$  (dashed) line shows the ideal case of complete agreement between estimated and measured values.

the diffuse component is rather skewed to the left (negative differences, MRM overestimation) on 28 March implying a slightly bad performance of the model in this case. The distribution of this component becomes broader in the case of the eclipse. Here, the MRM diffuse radiation is continuously underestimated. This is in agreement with the MBE values; on 28 March the MBE is very close to zero ( $-2.50\%$ ), while on the next day it becomes highly positive ( $+35.53\%$ ).

In conclusion, the RMSE and MBE statistics (Table 5) obtained very satisfactory values for the total horizontal irradiance on both days. There must be emphasized again that the 28 March was an almost cloudless day, while some cloudiness was developed over Athens on the eclipse day, 29 March, after the start of the phenomenon. This is the reason for increased values in both statistical estimators in the diffuse radiation component, as already stated above. Such a harsh test (eclipse with cloudy sky) for a broadband radiation model constitutes an ultimate validation of its performance. Therefore, an excellent efficiency of MRM v5 has been affirmed by the close agreement of the modeled and measured radiation components under “adverse” conditions.

To further show the capabilities of the MRM, Figure 6a and b are drawn. Figure 6a refers to the one-to-one comparison between the estimated and measured total horizontal irradiances on 28 March and Fig. 6b to the following day. It is easily seen that in both cases the data points are along the  $y=x$  line with minimum dispersion around it. The coeffi-

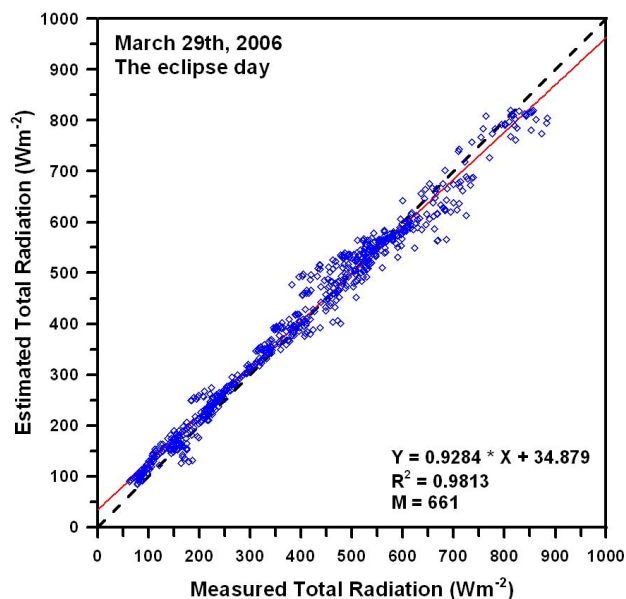


**Fig. 6b.** As in Fig. 6a, but on 29 March 2006.

cient of determination ( $R^2$ ) for the linear best fit curve to the data points as well as their number ( $M$ ) are also included in both diagrams. The slope of the linear best fit curves is the same (about 0.93) as well as the coefficient of determination (about 0.99) in both cases. This is an encouraging feature that MRM can work equally well under any circumstances.

#### 4 Conclusions

This study dealt with the validation of the Meteorological Radiation Model (MRM) developed by the Atmospheric Research Team of the National Observatory of Athens. Though the model, in its previous versions, has been checked in the past against measurements, this was the first time that the performance of the latest version 5 of the MRM algorithm was tested. To do this, a difficult case, such as the solar eclipse of 29 March 2006 over Athens with partly cloudy sky, was chosen. In running MRM the attention was paid on total radiation, as this is the component with the main interest in solar energy applications.

The test proved that the MRM v5 is an efficient broadband code capable of simulating solar irradiance at a location not only under clear sky conditions, but also with cloudy weather. Moreover, the mixture of such sky conditions with an eclipse event is done for the first time in the international literature as far as a solar broadband model is concerned. Although the results have a scientific and not practical value, they showed that MRM simulated the solar radiation level changes very well during the solar eclipse day of 29 March 2006 over Athens. Indeed, the RMSE and MBE statistical estimators were found to be  $7.64\%$  and  $-1.67\%$  on 29 March

**Table 5.** RMSEs and MBEs, in  $\text{Wm}^{-2}$ , for the MRM modeled total and diffuse horizontal radiation components together with their mean measured values for 28 and 29 March 2006 at ASNOA. The brackets in the RMSE and MBE columns indicate their values in %. The available 1-min data points are 661 on each date.

March 2006	Mean diffuse rad. ( $\text{Wm}^{-2}$ )	Mean total rad. ( $\text{Wm}^{-2}$ )	RMSE ( $\text{Wm}^{-2}$ and %)		MBE ( $\text{Wm}^{-2}$ and %)	
			Diffuse	Total	Diffuse	Total
28	87.83	560.61	22.66 (25.80)	29.68 (5.30)	-2.19 (-2.50)	+11.45 (+2.04)
29	175.63	395.17	85.33 (48.59)	30.21 (7.64)	+62.39 (+35.53)	-6.59 (-1.67)

for the simulated total solar radiation in comparison with the respective 5.30% and +2.04% for the previous clear day.

The efficiency of the MRM makes the model capable of handling other simulation situations as easily as in the case of a solar eclipse with even better results. Therefore, MRM can be used in a variety of applications, among which there can be atmospheric physics, photovoltaic studies, filling gaps of missing data from a solar radiation time series, solar thermal projects, agricultural studies, architectural designs. MRM can also be used in the derivation of a Solar Radiation (or Energy) Atlas over a region with as much accuracy as possible. This latter applicability makes MRM a precious tool in the energy sector.

### Latin symbols

$a, b, c, d$	numerical coefficients in the general transmittance function of various atmospheric constituents, dimensionless
$e_m$	partial water vapor pressure, in hPa
$e_s$	saturation vapor pressure, in hPa
$H$	station's altitude, in m
$I_{ex}$	normal incidence extra-terrestrial solar radiation on the $n_i$ -th day of the year, in $\text{Wm}^{-2}$
$I_c$	model estimated value of total or diffuse solar radiation, in $\text{Wm}^{-2}$
$I_b$	direct beam component of solar radiation, normal to the horizontal plane at the earth's surface, under clear sky conditions, in $\text{Wm}^{-2}$
$I_{cb}$	direct beam component of solar radiation, normal to the horizontal plane at the earth's surface, under cloudy sky conditions, in $\text{Wm}^{-2}$
$I_{cd}$	diffuse component of solar radiation, normal to the horizontal plane at the earth's surface, under cloudy sky conditions, in $\text{Wm}^{-2}$

$I_{cdm}$	ground reflected, atmospheric and cloud backscattered portion of the diffuse sky radiation under cloudy sky conditions, in $\text{Wm}^{-2}$
$I_{cds}$	portion of the diffuse sky radiation under cloudy sky conditions, singly scattered by the atmospheric constituents (molecules and aerosol particles), in $\text{Wm}^{-2}$
$I_{ct}$	total solar radiation, normal to the horizontal plane at the earth's surface, under cloudy sky conditions, in $\text{Wm}^{-2}$
$I_d$	diffuse component of solar radiation, normal to the horizontal plane at the earth's surface, under clear sky conditions, in $\text{Wm}^{-2}$
$I_{dm}$	ground reflected, atmospheric backscattered portion of the diffuse sky radiation under clear sky conditions, in $\text{Wm}^{-2}$
$I_{ds}$	portion of the diffuse sky radiation under clear sky conditions, singly scattered by the atmospheric constituents (molecules and aerosol particles), in $\text{Wm}^{-2}$
$I_m$	measured value of total or diffuse solar radiation, in $\text{Wm}^{-2}$
$I_o$	solar constant ( $1366.1 \text{ Wm}^{-2}$ )
$I_t$	total solar radiation, normal to the horizontal plane at the earth's surface, under clear sky conditions, in $\text{Wm}^{-2}$
$k$	empirical coefficient for cloudiness, dimensionless
$k^*$	empirical transmission coefficient for the singly scattered portion of the diffuse radiation under cloudy sky conditions, dimensionless
$m$	optical air mass, dimensionless
$m'$	pressure corrected optical air mass, dimensionless
$M$	number of available data points of total or diffuse solar radiation, for the RMSE or MBE statistical indicators estimation, dimensionless

$n$	daily measured sunshine duration, in h
$N$	daily maximum (astronomical) sunshine duration, in h
$n_i$	the day number of the year (1–365)
$P$	atmospheric pressure at station's altitude, in hPa
$P_o$	mean atmospheric pressure at sea level (1013.25 hPa)
RH	relative humidity at station's altitude, in %
$T$	air temperature at station's altitude, in K
$T_1$	equal to $T/100$ , in K
$T_a$	broadband transmittance function for aerosol total extinction (scattering and absorption), dimensionless
$T_{a,1.66}$	broadband transmittance function for aerosol total extinction, calculated for air mass $m=1.66$ , dimensionless
$T_{aa}$	broadband aerosol transmittance function due to absorption only, dimensionless
$T_{as}$	broadband aerosol transmittance function due to scattering only, dimensionless
$T_c$	cloud transmittance, dimensionless
$T_{CH_4}$	broadband transmittance function for CH <sub>4</sub> absorption, dimensionless
$T_{CO}$	broadband transmittance function for CO absorption, dimensionless
$T_{CO_2}$	broadband transmittance function for CO <sub>2</sub> absorption, dimensionless
$T_{mg}$	broadband transmittance function due to total uniformly mixed gases' (CO <sub>2</sub> , CO, N <sub>2</sub> O, CH <sub>4</sub> and O <sub>2</sub> ) absorption, dimensionless
$T_{N_2O}$	broadband transmittance function for N <sub>2</sub> O absorption, dimensionless
$T_{O_2}$	broadband transmittance function for O <sub>2</sub> absorption, dimensionless
$T_o$	broadband transmittance function for O <sub>3</sub> absorption, dimensionless
$T_r$	broadband transmittance function for Rayleigh scattering, dimensionless
$T_w$	broadband transmittance function for H <sub>2</sub> O absorption, dimensionless
$u_o$	total O <sub>3</sub> amount in a vertical column, in atm-cm
$u_i$	total amount in a vertical column for atmospheric uniformly mixed gases, in atm-cm ( $i = \text{CO}_2, \text{CO}, \text{N}_2\text{O}, \text{CH}_4, \text{O}_2$ )
$u_w$	water vapor total amount in a vertical column, in cm
$V$	horizontal visibility, in km

### Greek symbols

$\alpha_a$	atmospheric aerosol albedo due to atmospheric aerosol scattering, dimensionless
$\alpha_c$	corrective factor for multiple scattering between clouds and the surface of the earth, dimensionless
$\alpha_{cs}$	atmospheric albedo of a cloudy sky, dimensionless
$\alpha_g$	surface albedo, dimensionless
$\alpha_r$	atmospheric albedo due to molecular (Rayleigh) scattering, dimensionless
$\alpha_s$	atmospheric albedo of a cloudless sky, dimensionless
$\beta$	Ångström's turbidity parameter, dimensionless
$\beta'$	annual mean value of Ångström's turbidity parameter, dimensionless
$\Delta\beta$	seasonal deviation of the Ångström's turbidity parameter from its average value, dimensionless
$\Gamma$	day angle, in rad
$\theta_z$	solar zenith angle, in deg
$\phi$	station's geographical latitude, in deg

*Acknowledgements.* We would like to thank E. Plionis, Institute of Astronomy and Astrophysics, NOA, for his calculations of EM. Thanks are also owed to K. Eleftheratos for the operation of the Brewer spectrophotometer at the Academy of Athens.

Edited by: C. Zerefos

### References

- Atwater, M. A. and Ball, J. T.: A numerical solar radiation model based on the standard meteorological observations. *Sol. Energy*, 21, 163–170, 1978.
- Atwater, M. A. and Brown, P. S.: Numerical computations of the latitudinal variations of solar radiation for an atmosphere of varying opacity, *J. Appl. Meteorol.*, 13, 289–297, 1974.
- Badescu, V.: A new kind of cloudy sky model to compute instantaneous values of diffuse and global irradiance, *Theor. Appl. Climatol.*, 72, 127–136, 2002.
- Barbaro, S. B., Coppolino, S., Leone, C., and Sinagra, E.: An atmospheric model for computing direct and diffuse solar radiation, *Sol. Energy*, 22, 225–228, 1979.
- Berland, T. G. and Danilchenko, V. Y.: The continental distribution of solar radiation. *Gidrometeoizdat, Leningrad*, 1961.
- Bird, R. E. and Hulstrom, R. L.: Direct insolation models, US Solar Energy Research Institute Tech. Report, SERI/TR-335-344, Golden, Colorado, 1980.
- Bird, R. E. and Hulstrom, R. L.: A simplified clear-sky model for the direct and diffuse insolation on horizontal surfaces, US Solar Energy Research Institute Tech. Report, SERI/TR-642-761, 38, 1981.
- Davies, J. A., Schertzer, W., and Munez, M.: Estimating global solar radiation, *Boundary Layer Meteorol.*, 9, 33–52, 1975.
- Davies, J. A. and McKay, D. C.: Estimating solar irradiance and components, *Sol. Energy*, 29, 55–64, 1982.

- Davies, J. A., Abdel-Whahab, M., and McKay, D. C.: Estimating solar irradiation on horizontal surfaces, *Inter. J. Sol. Energy*, 2, 405–424, 1984.
- Ehnberg, J. S. G. and Bollen, M. H. J.: Simulation of global solar radiation based on cloud observations, *Sol. Energy*, 78, 157–162, 2005.
- Gu., L., Fuentes, J. D., Garstang, M., Da Silva, T. J., Heitz, R., Sigler, J., Shugart, H. H., Cloud modulation of solar irradiance at a pasture site in southern Brazil, *Agric. Forest Meteorol.*, 106, 117–129, 2001.
- Gueymard, C.: Critical analysis and performance assessment of clear sky solar irradiance models using theoretical and measured data, *Sol. Energy*, 51, 121–138, 1993a.
- Gueymard, C.: Assessment of the accuracy and computing speed of simplified saturation vapor equations using a new reference dataset, *J. Appl. Meteorol.*, 32, 1294–1300, 1993b.
- Gueymard C.: Direct solar transmittance and irradiance predictions with broadband model. Part I: detailed theoretical performance assessment, *Sol. Energy*, 74, 355–379, 2003.
- Ideriah, F. J. K.: A model for calculating direct and diffuse solar radiation, *Sol. Energy*, 26, 447–452, 1981.
- Iqbal, M.: An introduction to solar radiation, Academic Press, New York, 6, p. 119, 1983.
- Konratyev, K. Y. A.: Radiation in the atmosphere, Academic Press, New York, p. 912, 1969.
- Kambezidis, H. D. and Papanikolaou, N. S.: Total solar irradiance flux through inclined surfaces with arbitrary orientation in Greece: comparison between measurements and models, In Proceedings of XIV Assembly of EGS, 13–17, Barcelona, Spain, 1989.
- Kambezidis, H. D. and Papanikolaou, N. S.: Total solar radiation on tilted planes in Greece, *Technika Chronika B*, 10, 55–70 (in Greek), 1990a.
- Kambezidis, H. D. and Papanikolaou, N. S.: Solar position and atmospheric refraction, *Sol. Energy*, 44, 143–144, 1990b.
- Kambezidis, H. D., Psiloglou, B. E., Tsangassoulis, A. E., Logothetis, M. A., Sakellariou, N. K., and Balaras, C. A.: A methodology to give solar radiation on tilted plane from meteorological data, In Proceedings of ISES World Congress, edited by: Farkas, J., 99–104, Budapest, Hungary, 1993.
- Kambezidis, H. D. and Tsangassoulis, A. E.: Solar position and right ascension, *Sol. Energy*, 50, 415–416, 1993.
- Kambezidis, H. D., Psiloglou, B. E., and Synodinou, B. M.: Comparison between measurements and models of daily total irradiation on tilted surfaces in Athens, Greece, *Renew. Energ.*, 10, 505–518, 1997.
- Kasten, F. and Young, A. T.: Revised optical air mass tables and approximation formula, *Appl. Optics*, 28, 124–127, 1989.
- Leckner, B.: Spectral distribution of solar radiation at the Earth's surface-elements of a model, *Sol. Energy*, 20, 443–450, 1978.
- Lacis, A. A. and Hansen, J. E.: A parameterization for the absorption of solar radiation in the earth's atmosphere, *J. Atmos. Sci.*, 31, 118–132, 1974.
- Liu, B. Y. H. and Jordan R. C.: The interrelationship and characteristic distribution of direct, diffuse and total solar radiation, *Sol. Energy*, 4, 1–19, 1960.
- Lyons, T. J. and Edwards, P. R.: Atmospheric attenuation of solar radiation at Adelaide, *Q. J. R. Met. Soc.*, 101, 1013–1017, 1982.
- Maxwell, E. L., Myers, D. R., Rymes, M. D., Stoffel, T. L., Wilcox, S. M.: Producing a National Solar Radiation data base, in: Proceedings of the ISES Solar World Congress, Denver CO. Pergamon Press, 1007–1012, 1991.
- Maxwell, E. L.: METSTAT – The solar radiation model used in the production of the National Solar Radiation Data Base (NSRDB). *Sol. Energy*, 62, 263–279, 1998.
- Muir, L. R.: Comments on “The effect of the atmospheric refraction in the solar azimuth”, *Sol. Energy*, 30, p. 295, 1983.
- Muneer, T., Gul, M. S., Kambezidis, H. D., and Alwinkle, S.: An all-sky solar meteorological radiation model for the United Kingdom, In Proceedings CIBSE/ASHRAE Joint National Conf., CIBSE/ASHRAE (Eds), pp. 271–280, Harrogate, UK, 1996.
- Muneer, T.: Solar radiation and daylight models for the energy efficient design of buildings, 1st Edition, 65–70, Architectural Press, 1997.
- Muneer, T., Gul, M. S., and Kambezidis, H. D.: Solar radiation models based on meteorological data, In Proc. ISES World Congress, Taegon, Korea, 1997.
- Muneer, T., Gul, M. S., and Kambezidis, H. D.: Evaluation of all-sky meteorological model against long-term measured hourly data, *Energy Conv. and Manag.*, 39 (3/4), 303–317, 1998.
- Munro, D. S.: A surface energy exchange model of glacier melt and net mass balance, *Int. J. Climatol.*, 11, 689–700, 1991.
- Psiloglou, B. E., Santamouris, M., and Asimakopoulos, D. N.: On the atmospheric water-vapor transmission function for solar radiation models, *Sol. Energy*, 53, 445–453, 1994.
- Psiloglou, B. E., Santamouris, M., and Asimakopoulos, D. N.: Predicting the broadband transmittance of the uniformly-mixed gases (CO<sub>2</sub>, CO, N<sub>2</sub>O, CH<sub>4</sub> and O<sub>2</sub>) in the atmosphere for solar radiation models, *Renew. Energ.*, 6, 63–70, 1995a.
- Psiloglou, B. E., Santamouris, M., and Asimakopoulos, D. N.: On broadband Rayleigh scattering in the atmosphere for solar radiation modelling, *Renew. Energ.*, 6, 429–433, 1995b.
- Psiloglou, B. E., Santamouris, M., Varotsos, C., and Asimakopoulos, D. N.: A new parameterisation of the integral ozone transmission, *Sol. Energy*, 56, 573–581, 1996.
- Psiloglou, B. E., Santamouris, M., and Asimakopoulos, D. N.: Atmospheric broadband model for computation of solar radiation at the Earth's surface. Application to Mediterranean climate, *Pure Appl. Geophys.*, 157, 829–860, 2000.
- Spencer, J. W.: Fourier series representation of the position of the sun, *Search*, 2, p. 172, 1971.
- Suckling, P. W. and Hay, J. E.: Modelling direct, diffuse and total solar radiation for cloudless days, *Atmosphere*, 14, 298–308, 1977.
- Van Heuklon, T. K.: Estimating atmospheric ozone for solar radiation models, *Sol. Energy*, 22, 63–68, 1979.
- Walraven, R.: Calculating the position of the sun, *Sol. Energy*, 20, 393–397, 1978.
- Wilkinson, B. J.: An improved FORTRAN program for the rapid calculation of the solar position, *Sol. Energy*, 27, 67–68, 1981.
- Yang, K., Huang, G. W., and Tamai, N.: A hybrid model for estimation of global solar radiation, *Sol. Energy*, 70, 13–22, 2001.